https://doi.org/10.5194/egusphere-2025-325
Preprint. Discussion started: 13 February 2025

Accelerated export of terrestrial organic carbon to the Chukchi Sea since pre-industrial times

Bassem Jalali[1], Marie-Alexandrine Sicre[2], Jian Ren[1], Zhongqiao Li[1], Youcheng Bai[1] Liang Su[1], Vincent Klein[2], and Jianfang Chen[1,3]

[1] Key Laboratory of Marine Ecosystem Dynamics, Second Institute of Oceanography, Ministry of Natural Resources, Hangzhou 310012, China.
[2] LOCEAN, CNRS, Sorbonne Université, Campus Pierre et Marie Curie, Case 100, 4 Place Jussieu, 75032, Paris, France.
[3]State Key Laboratory of Satellite Ocean Environment Dynamics, Second Institute of Oceanography, Ministry of Natural Resources, Hangzhou 310012, China.

Corresponding authors: Jianfang Chen (jfchen@sio.org.cn) and Bassem Jalali (bassemfss@gmail.com)

Abstract

The on-going global warming is causing rapid changes in the carbon cycle of the Arctic. Yet the response of the Arctic to these environmental changes are not fully understood. In this study, we investigate bulk organic parameters (TOC, TN, $\delta^{13}C_{org}$, $\delta^{15}N$, C/N) and terrestrial n-alkanes (TERR-alkanes) from 19 surface sediments and 5 ^{210}Pb-dated sediment cores covering up to the last three centuries from the Chukchi Sea. Downcore profiles indicate increasing OC since the beginning of the Industrial Era in all cores. They also show higher TOC and TN values in southern Chukchi Sea cores coincident with decreasing $\delta^{13}C_{org}$ indicating an increasing contribution of terrestrial OC that is confirmed by TERR-alkanes. Comparison with regional paleo-records and instrumental data emphasize the key role of air temperature and sea ice cover on the OC cycle and vegetation of the surrounding landmasses.

Keywords: biomarkers, terrigenous organic carbon, Arctic region, pre-industrial Era

1. Introduction

The Arctic Ocean experiences increased organic carbon (OC) supply due to permafrost thawing, enhanced river discharge as well as increasing primary production triggered by sea ice retreat as a result of rising global temperatures (Holmes et al., 2021, Wolken, et al., 2021, Frey et al., 2021). The Arctic permafrost, accounting for about half of global soil OC pool (Hugelius et al., 2014), largely exceeds the atmospheric carbon pool, and can be rapidly mobilized upon

https://doi.org/10.5194/egusphere-2025-325
Preprint. Discussion started: 13 February 2025

warming and accelerated hydrological cycle, hence representing a "time-bomb" for global warming (Tanski et al., 2019; Fritz et al., 2017). Erosion of the coastal permafrost, representing ~34 % of the global coastline, is responsible for the release of 14 Tg of OC into the Arctic Ocean (Vonk et al., 2012; Couture et al., 2018). However, rivers are also major suppliers of terrestrial OC. While accounting for only 1 % of the global volume of seawater, the Arctic Ocean receives about 11 % (4300 km^3 $year^{-1}$) of the global river discharge, emphasizing the importance of continental runoff in the Arctic hydrologic cycle (McClelland et al., 2006; Walsh et al., 2020). Over the last decades, the increasing nutrient supply and the sea ice loss have led to a net primary production rise, the Eurasian Arctic being the most impacted region with an annual increase of 12.83 g C m^{-2} yr^{-1} (Frey et al., 2021). Biological uptake of atmospheric CO_2 is also remarkably high in marginal seas of the Pacific Arctic Region (PAR) such as the Chukchi Sea, one of the largest CO_2 sinks of the global ocean (Hill et al., 2018; Neeley et al., 2018; Tu et al., 2021).

Much can be learnt about marine-terrestrial interactions from the analysis of marine sediments. Bulk and molecular organic indicators have been widely used to characterize the OC content of sediments in the PAR (Fernandes and Sicre, 2000; Wang et al., 2019; Seki et al., 2021; Su et al., 2023; Bai et al., 2024). In this study, we investigate the spatial and temporal changes of the OC fingerprint using TERR-alkanes and commonly used bulk parameters, e.g. Total Organic Carbon (TOC), Total Nitrogen (TN), δ^{13}Corg, δ^{15}N and C/N ratio from 5 ^{210}Pb-dated sediment cores and 19 surface sediments from the Chukchi Sea (Figure 1a). We then examine the role of air temperature, sea ice concentration (SIC) and inland precipitation on changes recorded since ~1700 CE.

2 Material and methods

2.1 Surface and core sediments

Five sediment cores retrieved with a multi-corer and 19 surface sediments (0-2 cm) were obtained from the Chukchi shelf for this study (Figure 1a). The surface sediments were collected from the Chukchi shelf and Chukchi Plateau during the LV77 cruise on board the R/V Akademik M. A. Lavrentiev in 2016 and during the 11th Chinese National Arctic Research Expedition (CHINARE) in summer 2020 on board the R/V Xuelong 2.

Cores 14R09 (74.61ºN, 168.98ºW; 33 cm long, only the upper 13 cm are analyzed here; 184 m water depth) and ARC11-R1 (hereafter named R1, 74.64ºN, 169.13ºW; 15 cm long; 200 m water

https://doi.org/10.5194/egusphere-2025-325
Preprint. Discussion started: 13 February 2025

depth) were recovered from the northern Chukchi Sea during the CHINARE expeditions in 2014 on board the R/V Xuelong 1 and in 2020 on board the R/V Xuelong 2, respectively. Core ARC4-C07 (hereafter named C07, 72.54ºN, 165.33ºW, 20 cm long, 51 m water depth) was retrieved from the Chukchi shelf during the CHINARE expedition on board the R/V Xuelong 1 in summer 2010. Core 14S03 (72.23ºN, 157.05ºW; 51 cm long, 172 m water depth) was collected from the eastern Chukchi Sea during the CHINARE expedition in 2014 on board the R/V Xuelong 1 while core LV77-4 (69.20ºN, 174.9ºW; 44 cm long, 60 m water depth) was retrieved from the southwestern Chukchi Sea during LV77 cruise on board the R/V Akademik M. A. Lavrentiev in 2016. The ^{210}Pb and ^{137}Cs measurements (Astakhov et al., 2019; Bai et al., 2022; Su et al., 2023; Jalali et al., 2024) indicate that cores 14R09 and 14S03 cover the last three centuries while cores LV77-4, R1 and C07 span from the 1820s to 2014. These sediments were analyzed for bulk parameters and TERR-alkanes.

2.2 Bulk analyses

For Total Organic Carbon (TOC) and $\delta^{13}C_{org}$ analyses, about 0.5 g of freeze-dried and homogenized sediment was acidified using 1 mol L^{-1} HCl, heated in a water bath for over three days to remove carbonates. Samples were then washed three times using ultrapure water and placed in an oven at 60 ºC until complete dryness (Williford et al., 2007). About 4 mg was then placed into a silver capsule and analyzed for TOC on a CHNOS elemental analyzer coupled with an isotope ratio mass spectrometer (IRMS) Thermo, Delta V advantage. IAEA-CH3 (cellulose with $\delta^{13}C$ = -24.724‰) and Urea (CH4N2O; WC=20%) were used as standards for $\delta^{13}C_{org}$ and TOC measurements. Based on replicate analyses, the analytical errors for $\delta^{13}C_{org}$ and TOC were estimated to 0.2 ‰ and 0.1 %, respectively.

For total nitrogen (TN) and nitrogen isotopic composition ($\delta^{15}N$), between 10 and 20 mg of non-acidified freeze-dried sediments was placed into a silver capsule and analyzed on CHNOS elemental analyzer coupled with an isotope ratio mass spectrometer (IRMS) Thermo, Delta V advantage. We used Urea (CH_4N_2O; WC=20%) and IAEA-NO_3 (KNO_3; $\delta^{15}N$=4.7‰) as standards for TN and $\delta^{15}N$ measurements, respectively. The standard deviation of TN and $\delta^{15}N$ was estimated to 0.005 % and 0.2 ‰, respectively.

2.3 Terrestrial alkane analyses

https://doi.org/10.5194/egusphere-2025-325
Preprint. Discussion started: 13 February 2025

Lipids were extracted from 2 to 4 g of freeze-dried sediments using a mixture of dichloromethane/methanol (2:1 v/v). The total extracts were then separated into compound classes using silica gel chromatography (Ternois et al., 2000). The fraction containing n-alkanes was quantified using a gas chromatograph Agilent Technologies 7890 (30 m HP-1MS column, 0.25 mm in diameter, and 0.25 µm film thickness) coupled to mass spectrometry Agilent 262 Technologies 5975C inert XL. 5α-cholestane was added to the fraction as an external standard prior to Gas Chromatography-Mass Spectrometry (GCMS) analysis. The GC oven temperature was ramped from 60°C to 100°C (at 25°C/min), held for 10 min, and then from 100°C to 310°C (at 2°C/min). The injector temperature was set at 280°C and the carrier gas (helium) flow maintained at 1.2 ml/min. Detection of n-alkanes was achieved using selective ion monitoring based on mass spectral detection of selected ions (m/z 57 for n-alkanes). The same was done for the external standard 5α-cholestane (m/z 372). The relative abundances of n-alkanes were determined by comparing their peak areas to that of the external standard 5α-cholestane. The data were then normalized to dried sediment weight and TOC %.

2.4 Calculation of indices and composites

Several indices were calculated based on the n-alkanes distribution: the average chain length ACL, the carbon preference index (CPI_{alk}) and the P_{aq} using equations (1), (2) and (3), respectively:

(1)

$$ACL_{27\text{-}31} = (27 \times [C27] + 29 \times [C29] + 31 \times [C31]) / ([C27] + [C29] + [C31])$$

(2)

CPI_{alk} has been frequently used to assess the relative contribution of terrestrial sources (Kvenvolden, 1966).

$$CPI_{alk} = 0.5 \times ((C23+C25+C27+C29+C31) / (C22+C24+C26+C28+C30)) + ((C23+C25+C27+C29+C31) / (C24+C26+C28+C30+C32))$$

(3)

https://doi.org/10.5194/egusphere-2025-325
Preprint. Discussion started: 13 February 2025

P_{aq} = (C23+C25) / (C23+C25+C29+C31)

The relative contribution of Sphagnum, a common Arctic moss species, to n-alkanes was calculated from Vonk & Gustafsson (2009) using equation (4):

(4)

% Sphagnum = ((C25 / C25 + C29) - 0.07) / (0.72 - 0.07) ×100

Where 0.07 and 0.72 represent the two end-members of the C25 / (C25 + C29) ratio for higher plants and Sphagnum, respectively.

Composites of the $ACL_{27\text{-}31}$ and TERR-alkanes were calculated based on the individual reconstruction of the five cores. For TEER-alkanes, each time series was first normalized by subtracting its mean and dividing the residual by its standard deviation. The 5 normalized time series (original ones for $ACL_{27\text{-}31}$) were then merged chronologically to produce a single composite. The composite was then averaged into 10-yr bins for comparison with air temperature, sea ice concentration and inland precipitation.

3 Results

3.1 Bulk parameters

New $\delta^{13}C$, TN and $\delta^{15}N$ data generated from cores 14R09, 14S03 and LV77-4 and earlier published for R1 and C07 are shown in Figure 2 (Table S1). TOC from the 3 new cores (Figure 2a) can be found in Jalali et al. (2024). In all cores, TOC and TN values increase since the early 20th century, but this trend is more pronounced at the northern sites. The southern cores LV77-4, C07 and 14S03 show higher TN values (0.18 % and 0.25 %) than the northern cores (14R09 and R1) (0.08 % to 0.15 %) (Figure 2c). C/N in the two southern cores are similar and quite stable while lower and decreasing in the northern cores (Figure 2e).

The $\delta^{13}C$ values fluctuate between -22.2 and -21 ‰ in core LV77-4, from -25.4 to -22.7 ‰ in core 14S03 and from -25.4 to -22.6 ‰ in core 14R09 (Figure 2b). All records depict a decreasing trend since approximately 1850-1900 except for the northernmost station R1 where they show continuous increase and more depleted values. $\delta^{15}N$ values are broadly stable around 8 ‰ in cores LV77-4 and 14S03, except for the marked increase since the second half of the 20th century (Figure

https://doi.org/10.5194/egusphere-2025-325
Preprint. Discussion started: 13 February 2025

2d). This is in contrast with the rapid increase from 5.5 ‰ to 9.5 ‰, at the northern sites (R1, 14R09).

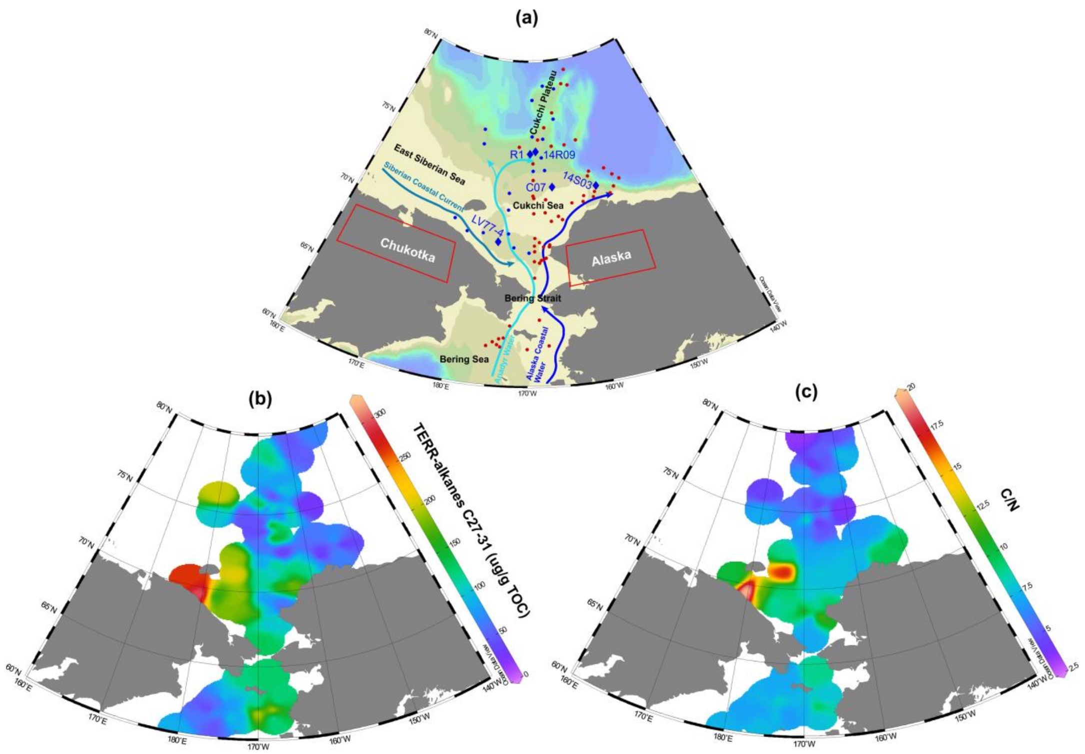

Figure 1: Map showing the location of the five cores (blue diamonds) and 19 surface sediments (blue dots). Surface sediments used for comparison are also shown (red dots) (Bai et al., 2024). Main ocean currents, geographical locations mentioned in the text and main seas of the western Arctic Ocean are also shown. Two red rectangles represent the grid points from which data of air temperature and precipitation have been extracted (discussed in detail in section 4.3). (b) and (c) combine TERR-alkanes and C/N data from all surface sediments (Table S2).

https://doi.org/10.5194/egusphere-2025-325
Preprint. Discussion started: 13 February 2025

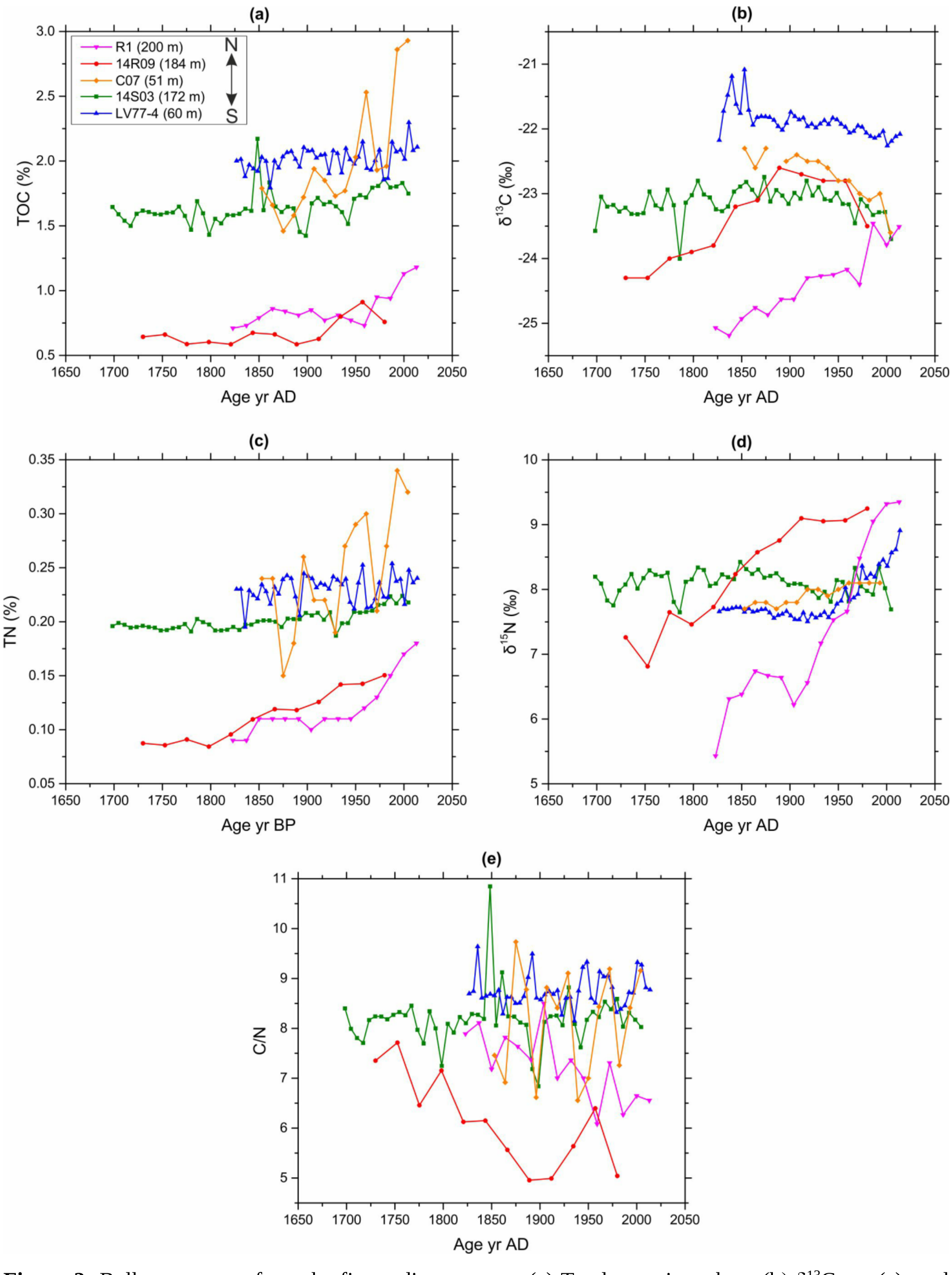

155
156 **Figure 2:** Bulk parameters from the five sediment cores. (a) Total organic carbon, (b) δ^{13}Corg, (c) total

https://doi.org/10.5194/egusphere-2025-325
Preprint. Discussion started: 13 February 2025

nitrogen (TN), (d) $\delta^{15}N$ and (e) carbon to nitrogen ratio (C/N) (see text). (a) Data published in Bai et al. (2022), Su et al. (2023) and Jalali et al. (2024). (b), (c), (d) and (e), data from the two cores R1 and C07 are from Bai et al. (2022) and Su et al. (2023). The same color coding of the cores is used for all figures.

3.2 TERR-alkanes

TERR-alkanes in surface sediments were more abundant in the southwestern Chukchi Sea on the path of Siberian Coastal Current (SCC, 266 to 303 µg/g TOC, Figures 1 and S1, Table S2). They showed intermediate values (190 µg/g TOC on average) in the rest of the Chukchi Shelf and lowest ones on the Chukchi Plateau (131 µg/g TOC on average).

Downcore TERR-alkane values are generally highly variable (Figure 3a, Table S1) ranging from 30 to 270 µg/g TOC at the northern core 14R09 with a steep decrease from the 1700s until about 1830, followed by a moderate increase towards present. Values in the other northern core R1 vary in a similar range (120 to 228 µg/g TOC) while in core C07 the range of variation is lower (32 to 107 µg/g TOC). In the southern core 14S03, TERR-alkanes display large amplitude fluctuations, notably until about 1870, spanning from close to 0 to 250 µg/g TOC. The other southern core LV77-4 shared similar characteristics over the overlapping period (from 1830 onwards) with values ranging from almost 0 to 400 µg/g TOC (Figure 3a).

ACL_{27-31} of the southern LV77-4 and 14S03 cores are again those exhibiting the largest fluctuations (Figure 3b), spanning between 28.4 and 29.3 with two deep drops around 1730 and 1820 in the longest 14S03 record. Values at the northern sites are broadly less variable except for core 14R09.

The P_{aq} ratio, used as an indicator of the contribution of aquatic plants, indicates stable values in the northern cores, around 0.4, and strongly variable ones in the southern 14S03 core until about 1870 (Figure 3c). Noteworthy is the decreasing trend of P_{aq} in LV77-4 while ACL_{27-31} concomitantly increases.

Finally, CPI_{alk} indicates similar values in all cores except at the northern site R1 where it is markedly lower (Figure 3d). The % sphagnum, ranging between 35 % and 90 %, exhibits similar features as P_{aq} including the steady decrease since 1850 accelerating after 1970 at LV77-4 (Figure 3e).

https://doi.org/10.5194/egusphere-2025-325
Preprint. Discussion started: 13 February 2025

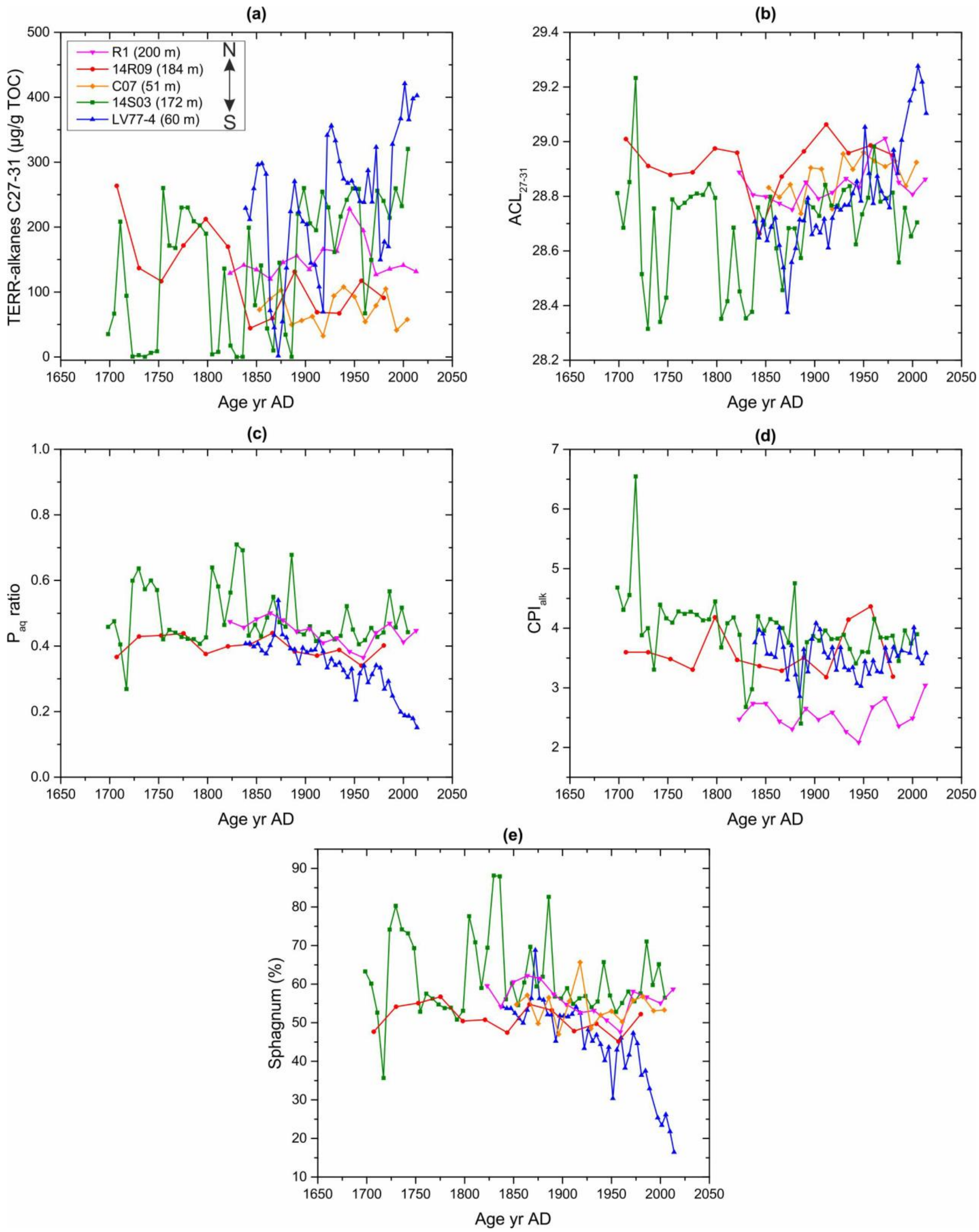

Figure 3: Downcore records from the five cores of (a) TERR-alkanes C_{27}-C_{31} (in ug/g TOC), (b) Average chain length of TERR-alkanes $ACL_{27\text{-}31}$, (c) P_{aq} ratio, (d) Carbon Preference Index CPI_{alk} and (e) percentage of Sphagnum to the total TERR-alkanes. The same color coding of the cores is used for all figures.

https://doi.org/10.5194/egusphere-2025-325
Preprint. Discussion started: 13 February 2025

4 Discussion

4.1 Spatial distribution of terrestrial biomarkers in the Chukchi Sea

In this section we compile the new TERR-alkane data from the 19 surface sediments with previously published TERR-alkanes data and bulk parameters from 107 surface sediments (Table S2; Su et al., 2023; Bai et al., 2024) to assess the spatial distribution of terrestrial OC in the modern Chukchi Sea (Figure 1b,c). Both high TERR-alkanes and C/N ratio demonstrate a strong contribution of terrestrial OC in the coastal sediments of the western Chukchi Sea (Figure 1) and eastern East Siberian Sea where the riverine influence is predominant, in agreement with the δ^{13}Corg data of Su et al. (2023). This is in contrast with the weaker terrestrial OC fingerprint at more northern latitudes reflecting higher primary production (pelagic and sympagic) and more distant terrigenous sources (Figure 1b,c).

4.2 Temporal changes of terrestrial carbon since pre-industrial times

4.2.1 Bulk parameters

The $\delta^{13}C_{org}$, combined with TOC and C/N ratio, have been widely used to discriminate marine from terrestrial OC in the Arctic Ocean (Fernandes et Sicre, 2000; Goñi et al., 2013; Tesi et al., 2016; Stein & MacDonald, 2004) because of distinct isotopic composition of terrestrial $\delta^{13}C_{org}$ (−26±1.5‰), phytoplanktonic (−24±3‰) and sea ice algal (−20.5±2‰) material. As shown in Figure 2a, the lower TOC of deep sediments (R1 and 14R09) stands out from the higher values of shallower and more southern cores (C07, 14S03 and LV77-4). The latter group also shows higher TN and C/N but heavier $\delta^{13}C_{org}$ values than deeper sediments (Figure 2b,c,e), reflecting mixed inputs of marine and terrestrial OC. Lowest $\delta^{13}C_{org}$ values around −22‰ suggest significant primary production possibly sustained by nutrient inputs at LV77-4. Another notable feature is the concomitant increase of $\delta^{13}C_{org}$ and C/N decrease in the deeper northern sediments that evidence a progressive growth of marine OC with respect to terrestrial OC in pre-industrial times, likely due to the retreat of sea ice (Figure 2b,e). This hypothesis is further supported by the steady increase of TN and δ^{15}N (Figure 2c,d). Our findings are in line with Jalali et al. (2024) based on sympagic and pelagic biomarkers (i.e. IP25, HBI-II, HBI-III, brassicasterol and dinosterol). Note that the downcore $\delta^{13}C_{org}$ record at all sites indicate a more or less pronounced decline since the early 20th century, reflecting enhanced export of terrestrial OC since 1850, except for the northernmost site R1 (Figure 2b).

https://doi.org/10.5194/egusphere-2025-325
Preprint. Discussion started: 13 February 2025

4.2.2 Terrestrial n-alkanes

Before 1850, TERR-alkanes in the 3 century-long southern 14S03 core show highly variable values with two major drops at 1720-1750 and 1800-1850 that are concurrent with sharp ACL_{27-31} decreases indicative of humid conditions in adjacent landmasses (Figure 3a,b). P_{aq} values point to a main contribution of submerged/floating freshwater aquatic macrophytes during these time-intervals that suggest an expansion of wetlands (Ficken et al., 2000) (Figure 3c). However, Sphagnum has a similar alkane distribution as macrophytes and thus similar P_{aq} values (Baas et al., 2000), but can be differentiated with the two-source end-members mixing model of $C_{25}/(C_{25}+C_{29})$ ratio of Vonk & Gustafsson (2009). Abrupt increase in this ratio up to 90 % between 1720-1750 and 1800-1850 leads to the conclusion of enhanced contribution of Sphagnum rather than expansion of wetlands (Figure 3e). In general, the CPI_{alk} show moderate decrease between 5 and 3 (Figure 3) that is consistent with rising marine production with retreating sea ice (Bröder et al., 2018).

After 1850, TERR-alkanes show large spatio-temporal variations across the study area and a long-term increase at cores LV77-4 and 14S03, not seen in the northern cores (Figure 3a), reflecting transport of terrestrial OC by the SCC and Alaska Coastal Water currents (Darby et al., 2009; Kim et al., 2017). This trend is consistent with the steady decline of $\delta^{13}C_{org}$. Simultaneously, the increase of ACL_{27-31}, most visible in the southern core site LV77-4, suggests the gradual establishment of drier conditions (Figure 3b) (Vogts et al., 2009). The P_{aq} and Sphagnum (%) underscore change of terrestrial OC supply to the Chukchi Sea (Figure 3c,e). The CPI_{alk} values, between 2 and 5 (Figure 3d), reflect mixed terrestrial and marine OC, except at northern site R1 where marine OC is markedly higher as testified by other bulk parameters.

https://doi.org/10.5194/egusphere-2025-325
Preprint. Discussion started: 13 February 2025

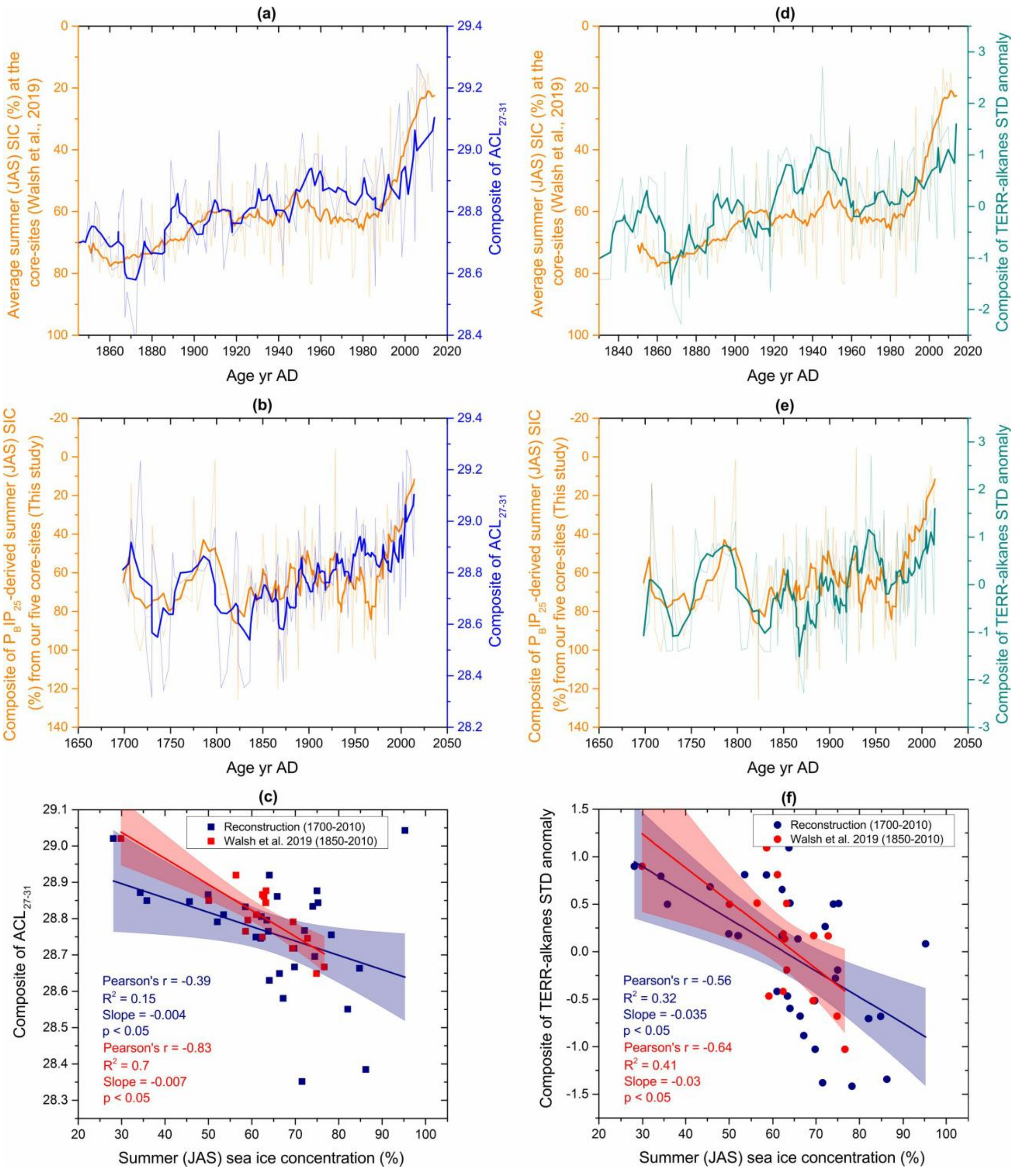

Figure 4: Comparison of the ACL_{27-31} composite obtained from our 5 core sites with (a) the average summer (JAS) sea ice concentration (SIC) from historical and satellite data at our core sites (Walsh et al., 2019) and (b) the composite of reconstructed SIC based on P_BIP_{25} data of our five sediment cores and the calibration of Jalali et al. (2024). (c) Cross plots and correlations calculated from 10 year bins (a) in red and (b) in blue. (d) Composite of TERR-alkane standardized anomalies from our 5 core sites with (d) average

https://doi.org/10.5194/egusphere-2025-325
Preprint. Discussion started: 13 February 2025

summer (JAS) SIC from historical and satellite data (Walsh et al., 2019) and (e) composite of reconstructed summer SIC based on P_BIP_{25} data and the calibration of Jalali et al. (2024). (f) Cross plots and correlations calculated from 10 year bins of the dataset (d) in red and (e) in blue. (a), (b), (d) and (e) Thick colored lines represent 10-year adjacent-averaging smoothing.

4.3 Factors controlling sedimentary terrestrial OC

4.3.1 Role of inland precipitation

The terrestrial hydrological cycle undergoes major changes due to global warming and its amplification in Polar Regions. Precipitation in the Arctic occurs mainly as snow that is released in summer into the river systems thereby contributing to the run-off and soil erosion in watersheds (Wagner et al., 2011). Rainfall has globally increased since 1950 and is expected to further increase in the future (Calvin et al., 2023), including in the Arctic region. However, modern observations and paleo-reconstructions also show a strong heterogeneity and seasonality of precipitation across the Arctic region (Linderholm et al., 2018; Walsh et al., 2020). We thus used gridded total annual precipitation from the Global Precipitation Climatology Centre (GPCC) at Alaska and Chukotka, for comparison with our records (Figure S2, Table S3). The obtained time series indicate a substantial increase of annual precipitation over the 20th century and a pronounced change at 1920-1960 that is not observed in the TERR-alkanes and ACL_{27-31} composites (Figure S2a,b), that shows no significant correlation with precipitation (Figure S2c,d).

4.3.2 Role of sea ice

Here we examine the role of SIC, using the historical and satellite observations from Walsh et al. (2019) at our core-sites (Figure 4a,d; Table S3) to compare them to TERR-alkanes and ACL_{27-31} composites over the same time period. Paleo-SIC were also calculated from the P_BIP_{25} data of our five cores and the calibration of Jalali et al. (2024) to generate a 300-year long paleo-SIC composite to extend this comparison to pre-industrial times (Figure 4b,e). Note that the proxy composite and observational summer (JAS) SIC time series are significantly correlated over the overlapping period (1850-2013) (Pearson's r = 0.72). Summer SIC indicates a gradual but moderate retreat of sea ice between 1850 and 1920 accelerating after 1980 (Figure 4a,d). This feature is also captured by the paleo-SIC composite, that also reveals generally higher SIC in pre-

https://doi.org/10.5194/egusphere-2025-325
Preprint. Discussion started: 13 February 2025

industrial times and a period of outstanding sea ice retreat between 1750 and 1800 in the southern Chukchi Sea (Figure 4b,e).

Both observed and reconstructed SIC time series show a significant negative correlation with the TERR-alkanes and ACL_{27-31} composites (Figure 4c,f). However, these correlations weaken for the 300-year long proxy composites, possibly due to uncertainties linked to the use of sea ice proxies. Nevertheless, these results support the key role of sea ice in the remobilization and transport of OC in the Arctic Ocean (Eicken et al., 2005; Darby et al., 2009) including in pre-industrial times as exemplified by the sea ice retreat between 1750 and 1800 coinciding with higher terrestrial OC.

Transport of terrestrial OC by sea ice involves the resuspension of the continental shelf sediments at shallow depth and their incorporation in newly formed sea ice and advection as far as the central Arctic (Darby et al., 2009). Land-fast ice can also modulate the thermal erosion in coastal areas and contribute to the supply of terrestrial OC (Irrgang et al., 2022; Nielsen et al., 2020). The role of sea ice in large-scale remobilization and transport of permafrost-derived OC has been evidenced during the warm Bølling Allerød of the last deglaciation (14,700 and 12,900 year BP) (Nogarotto et al., 2023). Overall, our 300-year records provide evidence of a significant link between sea ice and terrestrial OC export (TERR-alkanes) to the Chukchi Sea back in pre-industrial times, as far as in the 1700s. The negative relationship between sea ice and ACL_{27-31} is more tricky to interpret. It is possible that changes in ACL_{27-31} reflect changes of terrestrial OC sources/vegetation. However, based on previous studies, we can also speculate that with increased vegetation cover associated with sea ice retreat, enhanced evapotranspiration over the landmasses could be responsible for drier surface conditions reflected by ACL_{27-31} (Wrona et al., 2016; Bring et al. 2016).

4.3.3 Role of air temperature

Temperature influences the hydrological cycle of the Arctic through its effect on sea ice, snow and glacier melting as well as permafrost thaw. Several studies from Siberia and Alaska have shown increase in melting layers and thinning and/or retreating of the majority of glaciers, deepening of the active layers of permafrost and enhancing coastal erosion with rising temperature (Schuur et al., 2008; Vonk et al., 2012; Winski et al., 2018; Ding et al., 2019). Eurasian and North

https://doi.org/10.5194/egusphere-2025-325
Preprint. Discussion started: 13 February 2025

American river flows have reached unprecedented levels throughout the Holocene (Wagner et al., 2011) and in the most recent decades (Holmes et al., 2021).

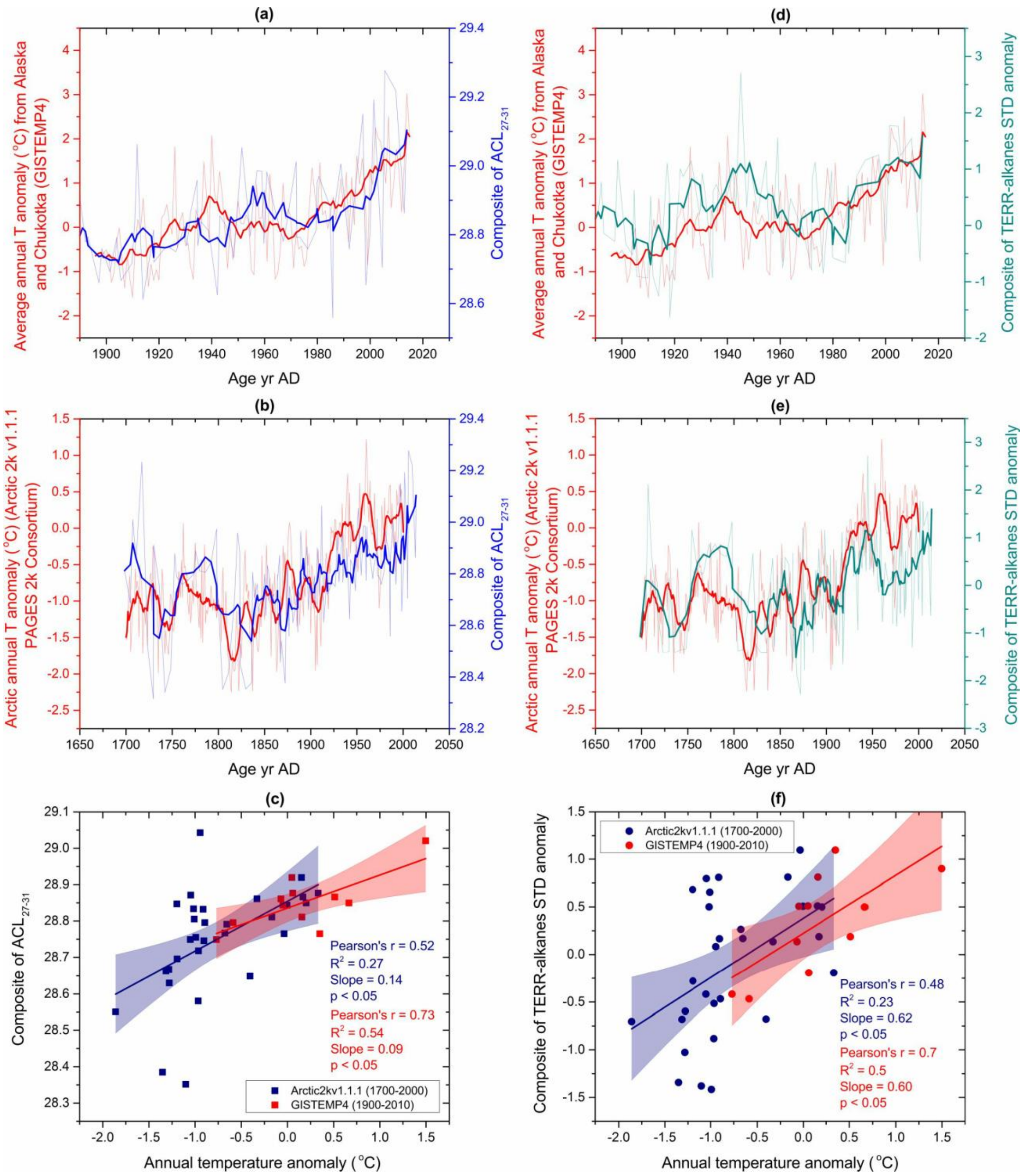

Figure 5: Plot of the ACL_{27-31} composite from our 5 core sites with (a) average air temperature anomalies (°C) over Alaska and Chukotka (https://data.giss.nasa.gov/gistemp/) and, (b) Arctic air temperature anomaly (°C) from PAGES 2k consortium (2013). (c) Cross plots and correlations calculated from 10 year

https://doi.org/10.5194/egusphere-2025-325
Preprint. Discussion started: 13 February 2025

bins of (a) in red and (b) in blue. Composite of TERR-alkane standardized anomalies obtained from our 5 core sites with (d) the average air temperature anomalies (°C) over Alaska and Chukotka (https://data.giss.nasa.gov/gistemp/) and (e) Arctic air temperature anomaly (°C) from PAGES 2k consortium (2013). (f) Cross plots and correlations calculated from 10 year bins of the dataset (d) in red and (e) in blue. (a), (b), (d) and (e) Thick colored lines represent 10-year adjacent-averaging smoothing.

In order to evaluate the role of temperature on terrestrial OC, we used instrumental annual air temperatures from the GISTEMPv4 database (Lenssen et al., 2024) at Alaska and Chukotka between 1896 and 2014 (Figure 5, Table S3). The paleo-reconstruction of annual temperature over the whole Arctic region (North of 60 °N) from PAGES 2k Consortium (2013) was also used for comparison of pre-industrial times (Table S3). The TERR-alkanes composite shows a significant positive correlation with annual air temperature, both for instrumental and proxy data (Figure 5d,e,f). A strong positive relationship is also evidenced with the ACL_{27-31} though weaker than with SIC (Figures 4a,c and 5a,c). These relationships also hold for pre-industrial times, but as for SIC, they weaken. Overall our results demonstrate the long-term increase of terrestrial OC export to the ocean and spreading polarwards highlighting the sensitivity of the Chukchi Sea to air temperature including in pre-industrial times.

5 Conclusions

Based on the distribution of bulk and molecular data of surface sediments and downcore records from the Chukchi Sea, we identified two areas: 1/ southern coastal shallow sediments characterized by high C and N reflecting mixed terrestrial OC eroded from the permafrost and marine-derived OC reflecting sustained planktonic production induced by high nutrient inputs of coastal waters and summer ice free conditions, 2/ northern deeper open sea sediments featuring a prevailing imprint of marine OC but increased terrestrial OC polarwards except for the northernmost site R1 where this influence remained minor.

The 300-year composite of TERR-alkanes indicates a long-term increase of terrestrial OC since the early 20th century picking up after 1980. This trend is paralleled by increasing ACL_{27-31} indicative of progressively dryer conditions. Our data also show that strong terrestrial OC export events occurred in pre-industrial times, e.g. between 1750 and 1800. They also show the strong control of temperature and summer sea ice in the export of terrestrial OC since the beginning of

https://doi.org/10.5194/egusphere-2025-325
Preprint. Discussion started: 13 February 2025

the 18^{th} century and its acceleration after 1980 reflecting the high sensitivity of the Arctic region to global warming and implications on the carbon cycle.

Data availability

Bulk and biomarker data from all surface sediments and the five sediment cores presented in this paper as well as time series of climate variables (air temperature, sea ice concentration and inland precipitation) used here for comparison, are available in the Supporting Information (Tables S1, S2 & S3).

Supplement

Supplemental material is available online at (link to be determined after submission).

Author contribution

BJ designed the study and wrote the paper with the help of MAS and JR. ZL, YB, SL and VK contributed to the bulk and biomarker analyses and the paper content. JC and ZL acquired funding from National Natural Science Foundation of China and made edits to the final version of the paper.

Competing interests

The authors declare that they have no conflict of interest.

Acknowledgments

This study was funded by the National Natural Science Foundation of China (Nos. 42076242, 42376243) and the Scientific Research Fund of the Second Institute of Oceanography, MNR, grant no. JB240. We thank the Centre National de la Recherche Scientifique (CNRS) for MAS salary. We are grateful to Qianna Chen, Jiaqi Wu and our colleagues of the biogeochemistry group for their kind help in the bulk and biomarker measurements.

https://doi.org/10.5194/egusphere-2025-325
Preprint. Discussion started: 13 February 2025

Bibliography

Astakhov A S, Bosin A A, Liu YG, Darin AV,Kalugin IA, Artemova AVandVologina: Reconstruction of ice conditions in the northern Chukchi Sea during recent centuries: geochemical proxy compared with observed data Quat. Int. 522 23–37, 2019.

Baas, M., Pancost, R., van Geel, B., & Damsté, J. S. S.: A comparative study of lipids in Sphagnum species. Organic Geochemistry, 31(6), 535-541, 2000.

Bai Y, Sicre M A, Ren J, Jalali B, KleinV, Li H and Chen J: Centennial-scale variability of sea-ice cover in theChukchi Sea since AD 1850 based on biomarker reconstruction Environ. Res. Lett. 17 044058, 2022.

Bai, Y., Sicre, M. A., Ren, J., Klein, V., Jin, H., & Chen, J.: Latitudinal distribution of biomarkers across the western Arctic Ocean and the Bering Sea: an approach to assess sympagic and pelagic algal production. *Biogeosciences Discussions*, *2023*, 1-34, 2024.

Bring, A., I. Fedorova, Y. Dibike, L.Hinzman, J.Mård, S. H.Mernild, T. Prowse,O. Semenova, S. L. Stuefer, andM.-K.Woo: Arctic terrestrial hydrology: A synthesis of processes, regional effects, and research challenges, J. Geophys. Res. Biogeosci., 121, 621–649, doi:10.1002/2015JG003131, 2016.

Bröder, L., Tesi, T., Andersson, A., Semiletov, I., & Gustafsson, Ö.: Bounding cross-shelf transport time and degradation in Siberian-Arctic land-ocean carbon transfer. Nature communications, 9(1), 806, 2018.

Calvin, K., Dasgupta, D., Krinner, G., Mukherji, A., Thorne, P. W., Trisos, C., ... & Hauser, M.: IPCC, 2023: Climate Change 2023: Synthesis Report. Contribution of Working Groups I, II and III to the Sixth Assessment Report of the Intergovernmental Panel on Climate Change [Core Writing Team, H. Lee and J. Romero (eds.)]. IPCC, Geneva, Switzerland. (No Title), 2023.

Couture, N. J., Irrgang, A., Pollard, W., Lantuit, H., & Fritz, M.: Coastal erosion of permafrost soils along the Yukon Coastal Plain and fluxes of organic carbon to the Canadian Beaufort Sea. Journal of Geophysical Research: Biogeosciences, 123(2), 406-422, 2018.

Darby, D. A., Ortiz, J., Polyak, L., Lund, S., Jakobsson, M., & Woodgate, R. A.: The role of currents and sea ice in both slowly deposited central Arctic and rapidly deposited Chukchi–Alaskan margin sediments. Global and Planetary Change, 68(1-2), 58-72, 2009.

Ding, Y., Zhang, S., Zhao, L., Li, Z., & Kang, S.: Global warming weakening the inherent stability of glaciers and permafrost. Science Bulletin, 64(4), 245-253, 2019.

Eicken, H., Gradinger, R., Gaylord, A., Mahoney, A., Rigor, I., & Melling, H.: Sediment transport by sea ice in the Chukchi and Beaufort Seas: Increasing importance due to changing ice conditions?. Deep Sea Research Part II: Topical Studies in Oceanography, 52(24-26), 3281-3302, 2005.

Ficken, K. J., Li, B., Swain, D. L., & Eglinton, G.: An n-alkane proxy for the sedimentary input of submerged/floating freshwater aquatic macrophytes. *Organic geochemistry*, *31*(7-8), 745-749, 2000.

Fernandes, M. B., & Sicre, M. A.: The importance of terrestrial organic carbon inputs on Kara Sea shelves as revealed by n-alkanes, OC and δ13C values. Organic Geochemistry, 31(5), 363-374, 2000.

Frey, K. E., Comiso, J. C., Cooper, L. W., Grebmeier, J. M., & Stock, L. V.: Arctic ocean primary productivity: The response of marine algae to climate warming and sea ice decline. Arctic Report Card, 2021.

Fritz, M., Vonk, J. E., & Lantuit, H.: Collapsing arctic coastlines. Nature Climate Change, 7(1), 6-7, 2017.

Goñi, M. A., O'Connor, A. E., Kuzyk, Z. Z., Yunker, M. B., Gobeil, C., & Macdonald, R. W.: Distribution and sources of organic matter in surface marine sediments across the North American Arctic margin. Journal of Geophysical Research: Oceans, 118(9), 4017-4035, 2013.

Hill, V., Ardyna, M., Lee, S. H., & Varela, D. E.: Decadal trends in phytoplankton production in the Pacific Arctic Region from 1950 to 2012. Deep Sea Research Part II: Topical Studies in Oceanography, 152, 82-94, 2018.

Holmes, R. M., Shiklomanov, A. I., Suslova, A., Tretiakov, M., McClelland, J. W., Scott, L., ... & Tank, S. E.: River discharge. Arctic Report Card, https://doi.org/10.25923/zevf-ar65, 2021.

https://doi.org/10.5194/egusphere-2025-325
Preprint. Discussion started: 13 February 2025

Hugelius, G., Strauss, J., Zubrzycki, S., Harden, J. W., Schuur, E. A., Ping, C. L., ... & Kuhry, P.: Estimated stocks of circumpolar permafrost carbon with quantified uncertainty ranges and identified data gaps. Biogeosciences, 11(23), 6573-6593, 2014.

Irrgang, A. M., Bendixen, M., Farquharson, L. M., Baranskaya, A. V., Erikson, L. H., Gibbs, A. E., Ogorodov, S. A., Overduin, P. P., Lantuit, H., Grigoriev, M. N., and Jones, B. M.: Drivers, dynamics and impacts of changing Arctic coasts, Nature Reviews Earth & Environment, 3, 39-54, 10.1038/s43017-021-00232-1, 2022.

Jalali, B., Sicre, M. A., Ren, J., Klein, V., Li, Z., Su, L., ... & Chen, J.: Reconstruction of sea ice variability in the Chukchi Sea during the last three centuries based on biomarker proxies. Environmental Research Communications, 6(9), 091013, 2024.

Kim, S. Y., Polyak, L., & Delusina, I.: Terrestrial and aquatic palynomorphs in Holocene sediments from the Chukchi–Alaskan margin, western Arctic Ocean: Implications for the history of marine circulation and climatic environments. *The Holocene*, *27*(7), 976-986, 2017.

Lenssen, N., Schmidt, G. A., Hendrickson, M., Jacobs, P., Menne, M. J., & Ruedy, R.: A NASA GISTEMPv4 observational uncertainty ensemble. Journal of Geophysical Research: Atmospheres, 129(17), e2023JD040179, 2024.

Linderholm, H. W., Nicolle, M., Francus, P., Gajewski, K., Helama, S., Korhola, A., ... & Väliranta, M.: Arctic hydroclimate variability during the last 2000 years: current understanding and research challenges. Climate of the Past, 14(4), 473-514, 2018.

McClelland, J. W., Déry, S. J., Peterson, B. J., Holmes, R. M., & Wood, E. F.: A pan‐arctic evaluation of changes in river discharge during the latter half of the 20th century. Geophysical Research Letters, 33(6), 2006.

Neeley, A. R., Harris, L. A., & Frey, K. E.: Unraveling phytoplankton community dynamics in the northern Chukchi Sea under sea‐ice‐covered and sea‐ice‐free conditions. Geophysical Research Letters, 45(15), 7663-7671, 2018.

Nielsen, D. M., Dobrynin, M., Baehr, J., Razumov, S., and Grigoriev, M.: Coastal Erosion Variability at the Southern Laptev Sea Linked to Winter Sea Ice and the Arctic Oscillation, Geophysical Research Letters, 47, 10.1029/2019gl086876, 2020.

Nogarotto, A., Noormets, R., Chauhan, T., Mollenhauer, G., Hefter, J., Grotheer, H., ... & Tesi, T.: Coastal permafrost was massively eroded during the Bølling-Allerød warm period. *Communications Earth & Environment*, *4*(1), 350, 2023.

PAGES 2k Consortium: Continental-scale temperature variability during the past two millennia. Nature geoscience, vol. 6, no 5, p. 339-346, 2013.

Schuur, E. A., McGuire, A. D., Schädel, C., Grosse, G., Harden, J. W., Hayes, D. J., ... & Vonk, J. E.: Climate change and the permafrost carbon feedback. Nature, 520(7546), 171-179, 2015.

Seki, O., Okazaki, Y., & Harada, N.: Assessment of long-chain n-alkanes as a paleoclimate proxy in the Bering Sea sediments. Progress in Oceanography, 198, 102687, 2021.

Stein, R., & MacDonald, R. W.: The organic carbon cycle in the Arctic Ocean. DOI 10.1007/978-3-642-18912, 2004.

Su L., Ren J., Sicre M. A., Bai Y., Zhao R., Han X. and Chen J.: Changing sources and burial of organic carbon in the Chukchi Sea sediments with retreating sea ice overrecent centuries. Climate of the Past 19 1305–20, 2023.

Tanski, G., Wagner, D., Knoblauch, C., Fritz, M., Sachs, T., & Lantuit, H.: Rapid CO2 release from eroding permafrost in seawater. Geophysical Research Letters, 46(20), 11244-11252, 2019.

Ternois, Y., Kawamura, K., Ohkouchi, N., & Keigwin, L.: Alkenone sea surface temperature in the Okhotsk Sea for the last 15 kyr. *Geochemical Journal*, *34*(4), 283-293, 2000.

Tesi, T., Semiletov, I., Dudarev, O., Andersson, A., & Gustafsson, Ö.: Matrix association effects on hydrodynamic sorting and degradation of terrestrial organic matter during cross‐shelf transport in the Laptev and East Siberian shelf seas. Journal of Geophysical Research: Biogeosciences, 121(3), 731-752, 2016.

https://doi.org/10.5194/egusphere-2025-325
Preprint. Discussion started: 13 February 2025

Tu, Z., Le, C., Bai, Y., Jiang, Z., Wu, Y., Ouyang, Z., ... & Qi, D.: Increase in CO2 uptake capacity in the Arctic Chukchi Sea during summer revealed by satellite-based estimation. Geophysical Research Letters, 48(15), e2021GL093844, 2021.

Vogts, A., Moossen, H., Rommerskirchen, F., & Rullkötter, J.: Distribution patterns and stable carbon isotopic composition of alkanes and alkan-1-ols from plant waxes of African rain forest and savanna C3 species. Organic Geochemistry, 40(10), 1037-1054, 2009.

Vonk, J. E., & Gustafsson, Ö.: Calibrating n-alkane Sphagnum proxies in sub-Arctic Scandinavia. Organic Geochemistry, 40(10), 1085-1090, 2009.

Vonk, J. E., Sánchez-García, L., Van Dongen, B. E., Alling, V., Kosmach, D., Charkin, A., ... & Gustafsson, Ö.: Activation of old carbon by erosion of coastal and subsea permafrost in Arctic Siberia. Nature, 489(7414), 137-140, 2012.

Wagner, A., Lohmann, G., & Prange, M.: Arctic river discharge trends since 7 ka BP. *Global and Planetary Change*, *79*(1-2), 48-60, 2011.

Walsh J. E., Chapman W. L., Fetterer F. and Stewart S.: Gridded Monthly Sea Ice Extent and Concentration, 1850 Onward, Version 2 NSIDC: National Snow and Ice Data Center, 2019.

Walsh, J. E., Ballinger, T. J., Euskirchen, E. S., Hanna, E., Mård, J., Overland, J. E., ... & Vihma, T.: Extreme weather and climate events in northern areas: A review. Earth-Science Reviews, 209, 103324, 2020.

Wang, K., Zhang, H., Han, X., & Qiu, W.: Sources and burial fluxes of sedimentary organic carbon in the northern Bering Sea and the northern Chukchi Sea in response to global warming. Science of the Total Environment, 679, 97-105, 2019.

Wegner, C., Bennett, K. E., de Vernal, A., Forwick, M., Fritz, M., Heikkilä, M., ... & Werner, K.: Variability in transport of terrigenous material on the shelves and the deep Arctic Ocean during the Holocene. Polar Research, 34(1), 24964, 2015.

Winski, D., Osterberg, E., Kreutz, K., Wake, C., Ferris, D., Campbell, S., ... & Handley, M.: A 400-year ice core melt layer record of summertime warming in the Alaska Range. Journal of Geophysical Research: Atmospheres, 123(7), 3594-3611, 2018.

Williford, K. H., Ward, P. D., Garrison, G. H., and Buick, R.: An extended organic carbon-isotope record across the Triassic–Jurassic boundary in the Queen Charlotte Islands, British Columbia, Canada, Palaeogeogr. Palaeoclimatol. Palaeoecol., 244, 290–296, https://doi.org/10.1016/j.palaeo.2006.06.032, 2007.

Wolken, G. J., Liljedahl, A. K., Brubaker, M., Coe, J. A., Fiske, G., Christiansen, H. H., ... & Streletskiy, D.: Glacier and permafrost hazards. Arctic report card https://doi.org/10.25923/v40r-0956, 2021.

Wrona, F. J., Johansson, M., Culp, J. M., Jenkins, A., Mård, J., Myers-Smith, I. H., ... & Wookey, P. A.: Transitions in Arctic ecosystems: Ecological implications of a changing hydrological regime. Journal of Geophysical Research: Biogeosciences, 121(3), 650-674, 2016.